Behavioral/Systems/Cognitive

Dynamic Interaction of Oscillatory Neurons Coupled with Reciprocally Inhibitory Synapses Acts to Stabilize the Rhythm Period

Akira Mamiya[1] **and Farzan Nadim**[2]

[1]Center for Molecular and Behavioral Neuroscience, Rutgers University, and [2]Department of Mathematical Sciences, New Jersey Institute of Technology, and Department of Biological Sciences, Rutgers University, Newark, New Jersey 07102

In the rhythmically active pyloric circuit of the spiny lobster, the pyloric dilator (PD) neurons are members of the pacemaker group of neurons that make inhibitory synapses onto the follower lateral pyloric (LP) neuron. The LP neuron, in turn, makes a depressing inhibitory synapse to the PD neurons, providing the sole inhibitory feedback from the pyloric network to its pacemakers. This study investigates the dynamic interaction between the pyloric cycle period, the two types of neurons, and the feedback synapse in biologically realistic conditions. When the rhythm period was changed, the membrane potential waveform of the LP neuron was affected with a consistent pattern. These changes in the LP neuron waveform directly affected the dynamics of the LP to PD synapse and caused the postsynaptic potential (PSP) in the PD neurons to both peak earlier in phase and become larger in amplitude. Using an artificial synapse implemented in dynamic clamp, we show that when the LP to PD PSP occurred early in phase, it acted to speed up the pyloric rhythm, and larger PSPs also strengthened this trend. Together, these results indicate that interactions between these two types of neurons can dynamically change in response to increases in the rhythm period, and this dynamic change provides a negative feedback to the pacemaker group that could work to stabilize the rhythm period.

Key words: **synaptic depression; synaptic dynamics; stomatogastric ganglion; oscillator; central pattern generator; dynamic clamp; motor system**

Introduction

Reciprocally inhibitory neuronal circuits are among the predominant building blocks involved in the generation of rhythmic patterns in the CNS (Kisvarday et al., 1993; Freund and Buzsaki, 1996; Marder and Calabrese, 1996). Numerous theoretical studies have examined how reciprocal inhibition gives rise to emergent network outputs, particularly rhythmic activity (Wang and Rinzel, 1992; Skinner et al., 1994; Van Vreeswijk et al., 1994; Nadim et al., 1999). However, reciprocal inhibition has been studied primarily within the context of simplified model networks or in static conditions, ignoring, for example, consequences of changes in the rhythm frequency and the resulting effects on synaptic and intrinsic dynamics. Recently, however, some computational studies have shown that in rhythmically active reciprocally inhibitory networks, the strength and timing of synapses can affect various aspects of the network activity, such as the oscillation frequency and the relative phasing between neurons (Nadim et al., 1999; Manor and Nadim, 2001; Taylor et al., 2002; Manor et al., 2003).

Dynamics of reciprocally inhibitory networks are not restricted to the intrinsic properties of the neurons involved. Many inhibitory synapses show short-term plasticity, thus adding an extra level of complexity to the network (Manor et al., 1997; Brody and Yue, 2000; Lewis and Maler, 2002; Mamiya et al., 2003). Although some modeling studies have shown the importance of the strength and timing of synapses in oscillatory neuronal networks and the possible significance of the interaction between synaptic strength and oscillation period, these issues have not been explored thoroughly in biological preparations. Thus, little is known about how such networks dynamically respond to changes in frequency in biologically realistic conditions.

This study investigates the interaction between oscillatory activity and synaptic dynamics in a biological network. The pyloric circuit of the spiny lobster (*Panulirus interruptus*) contains many pairs of neurons that produce rhythmic bursting activity. The pyloric rhythm (frequency, 0.5–2 Hz) is generated by a pacemaker group composed of an anterior burster (AB) and two pyloric dilator (PD) neurons. All follower pyloric neurons receive inhibitory synapses from the pacemaker neurons. The only feedback chemical synapse to the pacemaker neurons from the rest of the circuit is from the lateral pyloric (LP) neuron to the PD neurons. Previous studies have shown that synapses between the pacemaker group and the LP neuron show short-term depression (Manor et al., 1997; Rabbah et al., 2002). Thus, the LP neuron and the pacemaker group are connected by reciprocally inhibitory depressing synapses.

Received Oct. 4, 2003; revised April 27, 2004; accepted April 28, 2004.

This research was supported by National Institute of Mental Health Grant 60605–01 (F.N.). We thank Pascale Rabbah for her careful reading and comments on this manuscript.

Correspondence should be addressed to Farzan Nadim, Department of Biological Sciences, 101 Warren Street, Newark, NJ 07102. E-mail: farzan@njit.edu.

DOI:10.1523/JNEUROSCI.0482-04.2004

 0270-6474/04/245140-11$15.00/0

We studied the effects of changing the pyloric cycle period on this reciprocally inhibitory subnetwork in three sets of experiments. First, we showed how the membrane potential waveform of the LP neuron changes in response to altering the cycle period. We then explored how the changes in the LP neuron waveform affect the properties of the "LP to PD" synapse. Finally, we examined how the changes in the properties of this feedback synapse to the pacemaker group, in turn, affect the oscillation period. Our results indicate that the strength and timing of the feedback synapse dynamically change in response to increases in the oscillation period and that these changes provide a negative feedback that stabilizes the cycle period.

Materials and Methods

Preparation and identification of the neurons. Adult spiny lobsters, *Panulirus interruptus* (Don Tomlinson, San Diego, CA), were used in all of the experiments. The stomatogastric nervous system (STNS) was isolated using standard procedures (Selverston et al., 1976; Mamiya et al., 2003). The isolated STNS was pinned down on a Sylgard-coated Petri dish and superfused throughout the experiments with chilled (16°C) physiological saline containing (in mM): 479.0 NaCl, 12.9 KCl, 13.7 $CaCl_2 \cdot 2H_2O$, 10.0 $MgSO_4 \cdot 7H_2O$, 3.9 $NaSO_4 \cdot 10H_2O$, 11.2 Trizma base, 5.1 Maleic acid, pH 7.45.

Pyloric neurons were identified according to their stereotypical axonal projections in identified nerves using conventional techniques (Selverston et al., 1976; Mamiya et al., 2003). Pyloric activity was monitored extracellularly with stainless steel wire electrodes from identified nerves. Extracellular signals were amplified with a differential AC amplifier (model 1700; A-M Systems, Carlsborg, WA). Intracellular recordings were made by impaling the somata with glass microelectrodes filled with 0.6 M K_2SO_4 plus 20 mM KCl (for identification of neurons and intracellular recordings; resistance, 30–35 MΩ) or 3 M KCl (for current injection only; resistance, 8–12 MΩ). All intracellular recordings were done with Axoclamp 2B amplifiers (Axon Instruments, Foster City, CA).

Comparison of the shape of the LP neuron waveform at different pyloric periods. To build a library of LP neuron waveforms at different pyloric periods, we recorded intracellularly from the LP neuron during an ongoing pyloric rhythm and injected various levels of DC (−20 to +4 nA) into one of the pacemaker group neurons (AB or PD) to change the rhythm period. Recorded voltage traces were low-pass filtered at 10 Hz (to remove action potentials) and divided into single cycles. To compare the shape of the single cycle waveforms across different periods and different preparations, each waveform was normalized both in amplitude (from a minimum of 0 to a maximum of 1) and in time (to a phase = time/period between 0 and 1). Within each preparation, collected waveforms were grouped according to period into 25 msec bins and averaged within each bin. We did not average the waveforms across preparations, because LP waveforms from different preparations varied in shape even when they had the same period. Bins that had fewer than three waveforms were not used for the comparison of the waveforms. We analyzed 275 average waveforms collected from 14 preparations. For principal component analysis, each average waveform was resampled at 100 points. For all other analyses, waveforms were sampled at 1000 points.

Principal component analysis (PCA) is a mathematical transformation that can be applied to a set of possibly correlated variables to find a smaller set of uncorrelated (orthogonal) variables (principal components) that can account for the majority of the original variances. When PCA is applied to a data set, it produces principal components (PCs) in the order of the variance within the data set, with the first PC having the maximum variance (Glaser and Ruchkin, 1976). We performed PCA on the LP waveform data embedded in a 100-dimensional space (each dimension corresponding to one sample point of the waveform) to find a few variables that can account for most of the variance seen in the waveform data set. This procedure enabled us to look for features that were changing greatly between the waveforms.

Construction of the LP waveform set and measuring postsynaptic potential in the PD neuron. Although the shape of the LP waveform differed between preparations, all waveforms changed in a consistent manner when the pyloric period was changed. We therefore chose one representative preparation and used averaged waveforms (see above for construction of the average waveforms) that corresponded to five different pyloric periods (550, 750, 950, 1150, and 1350 msec) as an LP waveform set.

Synaptic potentials were measured after abolishing the pyloric activity to allow for better control of the membrane voltage. This was done by bath application of 0.1 μM tetrodotoxin (TTX; Biotium, Hayward, CA) to block descending inputs to the stomatogastric ganglion. This also blocked action potentials and action potential-mediated synaptic transmission in the ganglion. In this study, we focused on graded synaptic transmission, which has been shown previously to be important and sufficient for the production of the triphasic pyloric rhythm (Graubard, 1978; Raper, 1979). To activate the LP to PD synapse, the LP neuron was voltage clamped with two electrodes, LP waveforms that corresponded to different pyloric periods were periodically played back at the corresponding period, and the postsynaptic potential (PSP) was recorded from the PD neurons in current-clamp mode. Each waveform was applied from a holding potential of −60 mV (the typical resting potential of the LP neuron) with a fixed amplitude of 30 mV for 10 cycles. This protocol was repeated five times for each waveform, and the resulting PSPs were averaged over the five repetitions. A 30 sec interval was allowed between each of the five repetitions to allow the synapse to completely recover from depression. The resting potential of the PD neuron did not change during the experiments and was in a range of −55 mV ± 3 mV in all preparations.

Activation of the artificial synapse. To study how the changes in the LP to PD PSP affect the pyloric period, we replaced the biological LP to PD synaptic current with an artificial synapse and observed the change in the rhythm period at different strengths and cycle phases of the artificial synapse. The artificial synapse was activated using the dynamic-clamp technique (Sharp et al., 1993; Manor and Nadim, 2001). Intracellular recordings were made from the LP and the two PD neurons during the ongoing pyloric rhythm, and the biological LP to PD synapse was removed by hyperpolarizing the LP neuron. One of the two PD neurons was impaled with two electrodes, one for recording the membrane potential and the other for current injection. The other PD neuron was impaled only with a current injection electrode in bridge mode. The artificial synaptic current was calculated on the basis of the membrane potential of the PD neuron measured by the recording electrode, reversal potential of the synapse (set at −75 mV), and the conductance of the synapse. The same synaptic current was injected into both PD neurons through the current injection electrodes. The artificial synapse was activated for 20 sec, and the average periods of the 10 cycles immediately before and the 10 cycles during the activation were compared. For calculation of the average period during the activation of the synapse, the first three cycles after the activation of the synapse were excluded to remove any transient effects.

The artificial synaptic current was activated periodically during each cycle of the PD neuron oscillation and was set to 0 between activations. The synapse was always activated at a prescribed phase (for example, 0.3) of the PD neuron oscillation for a preset duration (200 msec, unless specified otherwise). The phase of the synaptic activation was calculated according to the period of the previous cycle of oscillation using the PD neuron burst onset as the reference point. Thus, if the activation phase was set at 0.3 and the previous cycle period was 900 msec, the synapse was activated 270 msec (=0.3 × 900 msec) after the first action potential of the PD neuron burst for a duration of 200 msec. If the PD neuron cycle period then changed to 960 msec, the synapse was activated at 288 msec (=0.3 × 960 msec) after the first action potential of the PD neuron (still for 200 msec) in the next cycle. Thus, the activation time of the synapse was adaptively adjusted according to the PD neuron cycle period to maintain a constant phase of the synaptic activation. This protocol was chosen to mimic the activation of the biological LP to PD synapse at each phase.

The shape of the conductance of the artificial synapse was approximated with a 200 msec wide triangle (ramp) that peaked at 0, 100, or 200 msec. The synapse was activated at four different phases (0.2, 0.3, 0.4, and 0.5) of the rhythm cycle. The strength of the synapse was varied in three steps (0.5, 1.0, and 2.0 nS) with values chosen to produce approximately the same size IPSP in the PD neurons as the biological LP to PD synapse.

Recording, analysis, and statistics. All intracellular recordings were digitized at 4 kHz and stored on a personal computer using a PCI-MIO-16E-1 board (National Instruments, Houston, TX) and custom-made recording software (http://stg.rutgers.edu/software/software.htm) written in LabWindows/CVI (National Instruments). Low-pass filtering of traces was done with a custom-made analysis program written in LabWindows/CVI. All other analyses, such as the waveform comparison, principal component analysis, PSP peak and amplitude detection, and the calculation of the period change were done by custom-made programs written in Matlab (MathWorks, Natick, MA). Statistical tests were done using SAS (SAS Institute, Cary, NC).

Results

In the rhythmically active pyloric network (six neuron types; cycle period, 0.5–2 sec), the pacemaker neurons (AB and two PDs) are reciprocally connected to the single follower LP neuron by depressing inhibitory synapses (Fig. 1*A*,*B*). The LP to PD synapse is the sole chemical feedback synapse from the rest of the pyloric network to the pacemaker neurons. As such, it is the primary synaptic candidate for affecting the rhythm produced by the pacemaker neurons (Manor et al., 1997; Weaver and Hooper, 2003a). In the present study, we investigated how the LP to PD feedback synapse dynamically changes in response to changes in the pyloric cycle period and how these changes, in turn, affect the cycle period.

The present study was done in three steps. First, we characterized how, during oscillations, the shape of the LP membrane potential waveform changed in response to changes in the pyloric rhythm cycle period. The pyloric cycle period was changed by current injection into the pacemaker neurons, the LP neuron was recorded intracellularly, and a library of LP waveforms corresponding to different rhythm periods was collected. Waveforms in the library were divided into single cycles, low-pass filtered, and indexed by their cycle period. Second, we measured how changes in the LP waveform affected the properties of the LP to PD synapse. We abolished the ongoing pyloric rhythm by bath application of TTX, voltage clamped the LP neuron, and periodically played back the prerecorded LP waveforms from the library at their corresponding cycle periods. The voltage variations of the LP neuron activated the LP to PD synapse, and we recorded the PSPs in the PD neurons. In the third and final step, we investigated how the changes in the PD neuron PSP affect the pyloric cycle period. These experiments were done by removing the biological LP to PD synapse during the ongoing pyloric rhythm and replacing it with an artificial synapse using the dynamic-clamp technique (Sharp et al., 1993; Manor and Nadim, 2001). The artificial synapse was applied periodically at different phases of the cycle and with different strengths, and the PD neuron activity was measured before, during, and after the activation of the artificial synapse. These three steps tracked the influence of the oscillatory activity in the pyloric pacemaker neurons on the follower LP neuron and examined the feedback effects from the LP neuron to the pacemaker neurons within a biologically realistic context.

Characterization of changes in the LP waveform in response to changes in the pyloric rhythm period

In the first step of this study, we characterized how the LP waveform changes in response to changes in the period of the pyloric rhythm. We changed the rhythm period by injecting DC into the pacemaker neurons (AB and PD) and recorded from the LP neuron intracellularly. The top traces in Figure 2*A* show an example of the LP neuron voltage trace recorded in control and when −20 nA DC was injected into the AB neuron to slow the pyloric rhythm. In this study, we focused on the graded component of the synaptic transmission, which has been shown to be important and sufficient to produce the triphasic pyloric rhythm (Graubard, 1978; Manor et al., 1997). Therefore, we low-pass filtered the voltage traces at 10 Hz to remove the action potentials from the waveforms (Fig. 2*A*, bottom traces).

To compare the shape of the waveforms at different periods, the recorded waveforms were cut into single cycles, sampled at 1000 points, and normalized both in amplitude (from a minimum of 0 to a maximum of 1) and in time (to obtain a phase = time/period between 0 and 1). Within each preparation, waveforms with similar period had similar shapes. We therefore

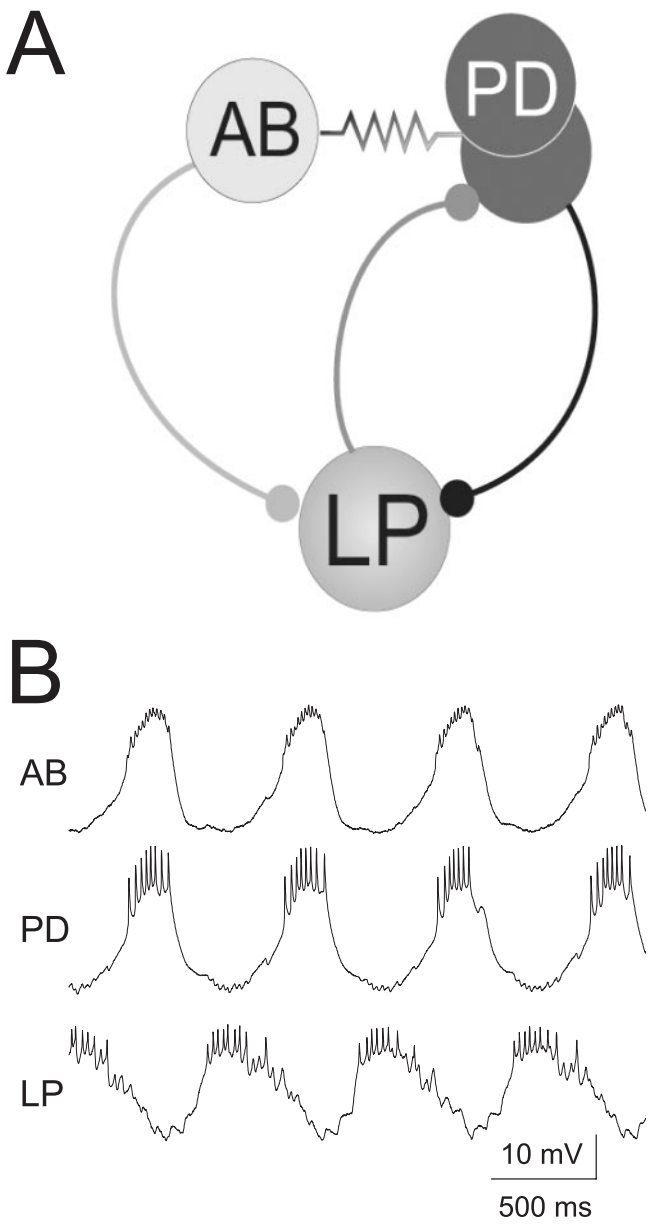

Figure 1. The pacemaker (AB and two PD) neurons and the LP neuron are connected by reciprocally inhibitory synapses. *A*, Circuit diagram shows the connectivity among the AB, PD, and LP neurons. The AB and PD neurons are connected with strong electrical connections. The AB–PD neurons and the LP neuron are connected by reciprocally inhibitory synapses. The LP to PD synapse is the sole chemical feedback synapse from the rest of the pyloric network to the pacemaker neurons. *B*, Intracellular voltage traces from the AB, PD, and LP neurons. The AB and PD neurons are coactive because of their strong electrical coupling. These two neurons oscillate in antiphase with the LP neuron.

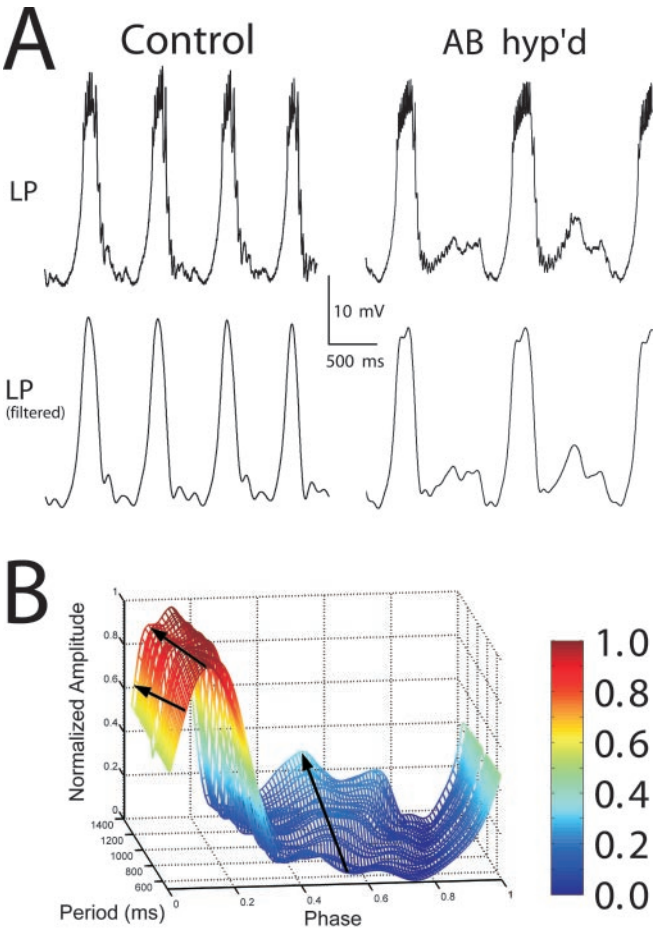

Figure 2. Changes in the LP waveform in response to altering the pyloric rhythm period. *A*, Top, An example of the LP neuron voltage trace recorded when either 0 nA (Control) or −20 nA DC was injected into the AB neuron to slow the rhythm period. Bottom, The same LP neuron voltage traces after the low-pass filtering at 10 Hz to remove the action potentials. *B*, Average LP waveforms from one preparation ranging in period from 550 to 1350 msec shown using phase (time/period of the waveform). Waveforms were grouped according to their period using 25 msec bins and averaged. The entire length of the three arrows point to three features of the LP waveforms that changed the most in response to the change in the rhythm period (from left to right: trough-to-peak slope, initial peak, and second smaller peak). Colors denote normalized amplitude. AB hyp'd, AB neuron hyperpolarized by DC injection.

grouped the waveforms according to their period using 25 msec bins and averaged the waveforms in the same bin. Figure 2*B* shows the average LP waveforms from one preparation ranging in period from 550 to 1350 msec. As seen in this Figure, the average waveform from each preparation always changed relatively smoothly in response to changes in the pyloric period, and there was no drastic qualitative change in the shape of the waveform.

Even though LP waveforms with similar period had similar shapes in individual preparations, the LP waveforms varied in shape across preparations even when the periods were the same. Therefore, we did not average waveforms across preparations. Despite the differences in shape, however, all LP waveforms seemed to change according to a fixed pattern when the rhythm period was changed. In particular, as the period was increased, the LP waveform began to peak at an earlier phase, the trough-to-peak slope of the waveform became steeper (in phase), and a second smaller peak started to appear (Fig. 2*B*, arrows). The appearance of this second peak seemed to be attributable to the fact that, with long cycle periods, the LP neuron would begin to rebound from the inhibition from the pacemaker neurons to initiate a burst. However, this premature burst initiation would be suppressed by inhibition from the pacemaker neurons in the next cycle (Fig. 2*A*, top right LP neuron trace).

To understand the general patterns of change in the LP waveform with period, we first examined the overall variability in the waveforms. We performed principal component analysis on 275 average waveforms collected from 14 preparations to see whether the variability in the waveforms could be described by a small number of parameters. The first two PCs accounted for 52.7% of the overall variance in the waveforms. The first PC accounted for 35.8% of the variance and showed a high negative correlation with the period of waveforms ($r = -0.594$; $n = 275$; $p < 0.0001$) (Fig. 3*A*). Thus, a large amount of variability in the waveforms might be attributable to a linear change in the waveform shape in response to changes in period. The significant negative correlation suggested that, as the period became longer, a large proportion of the overall change in the waveform was an increase by a value proportional to the negative of the first PC. To clarify what type of variation in the waveform was represented by the first PC, we plotted the negative of the first PC [red curve marked -(PC1)] together with the mean of all average waveforms (Fig. 3*B*).

Each point on the curve –(PC1) shows the weight of the corresponding point of LP waveforms used for the calculation of the negative of the first principal components. Because these values are weights, they have no units. The peaks and valleys of –(PC1) correspond to the positive and negative peaks of the weight. Thus, the points on the waveform in the same position as the peaks had large positive contribution, whereas those in the position of the valleys had large negative contribution to the PC. When the period was increased, –(PC1) also increased; thus, the value of the waveform points near the peak of –(PC1) was increasing, and those near the valley were decreasing. The overlay of the waveform and –(PC1) in Figure 3*B* indicated a variation in the waveforms on the basis of the location of the initial peak and the amplitude of the second peak. This was consistent with our initial observation that as the period became longer, the LP waveform shifted its peak to an earlier phase, its initial slope became steeper (in phase), and a second peak started to appear (Fig. 2*B*). Gray boxes are placed in a position that corresponds to the two largest positive peaks. To ensure that the variations indicated by the first principal component were consistent across preparations, we marked the positions (Fig. 3*B*, shaded regions) corresponding to the two largest positive peaks of –(PC1) and performed a visual inspection of average waveforms recorded from each preparation in these regions. This inspection confirmed that the values of waveform points within these regions were indeed increasing when the period was increased.

Figure 3, *C* and *D*, shows an example of changes in the LP waveform as the cycle period was changed from 525 to 1150 msec in one experiment. The parts of the waveforms shown in Figure 3, *C* and *D*, corresponded to the shaded regions in *B*. As the cycle period was increased, the LP waveform began to peak at an earlier phase and, as a result, the trough-to-peak slope of the waveform became steeper in phase (Fig. 3*C*). Moreover, a second smaller peak started to appear in the waveform (Fig. 3*D*). This shift of the peak and the change in the slope was seen in all 14 preparations. Most preparations (9 of 14) developed a clear second peak when the period was increased.

The first PC also suggested that other features of the waveform such as duty cycle (defined as the width of the waveform at half amplitude) might decrease slightly and burst width (the width of the burst of action potentials as approximated by the width of the

waveform at 75% amplitude) might not change as much as the waveform period is changed. This followed from the observation that the decrease in the values of waveform points as suggested by the large valley (near phase 0.4) of –(PC1) would act to decrease the duty cycle slightly and thus keep the burst width constant.

The second PC accounted for 16.9% of the variance in the waveforms and showed very little correlation with period ($r = 0.163$; $n = 275$; $p < 0.00667$; data not shown), reflecting the fact that LP waveforms can differ greatly across preparations even when their periods are the same.

To further confirm that these changes were consistent across preparations and to quantify the patterns of change, several parameters that described the above changes were plotted against the cycle frequency and the cycle period for all average waveforms ($n = 275$) obtained from 14 different preparations (Figs. 4, 5). To see whether the parameters describing the LP waveform correlated with period with constant phase (such as the peak of a sine wave) or constant time delay (such as the peak of an action potential in a tonically spiking neuron), we measured all parameters both in phase and in time. Parameters measured in phase were plotted against the cycle frequency (Figs. 4*A*, 5, left panels), and parameters measured in time were plotted against the cycle period (Figs. 4*B*, 5, right panels). This representation would show parameters with a constant time delay to be plotted as a line (passing through the origin) in a phase-representation plot and parameters with a constant phase to be plotted as a line (passing through the origin) in a time-representation plot (Hooper, 1997a). The shift of the waveform peak was measured as the phase or time from the half-amplitude point of the waveform to the initial peak. We chose the half-amplitude point instead of the minimum point of the waveform because some waveforms had several troughs and it was not easy to identify a single clear minimum point. The change in the trough-to-peak slope was measured as the phase or time it took for the waveform to rise from 25 to 75% of the maximum amplitude. Again, we did not measure from minimum to maximum because of the lack of a clear minimum. To quantify the development of the second peak in the waveform, we found the waveform peaks in the part of the waveform between phases 0.5 and 0.8 (Fig. 3*D*, corresponding shaded area in *B*). This range was chosen because the second peak always appeared in this range, whereas the first peak never occurred in this range. We also quantified parameters corresponding to duty cycle and burst width. Note that we used the width of the waveform at 75% amplitude to represent the burst width. These parameters were chosen because they are believed to be important for graded synaptic transmission and the overall activity of the pyloric circuit.

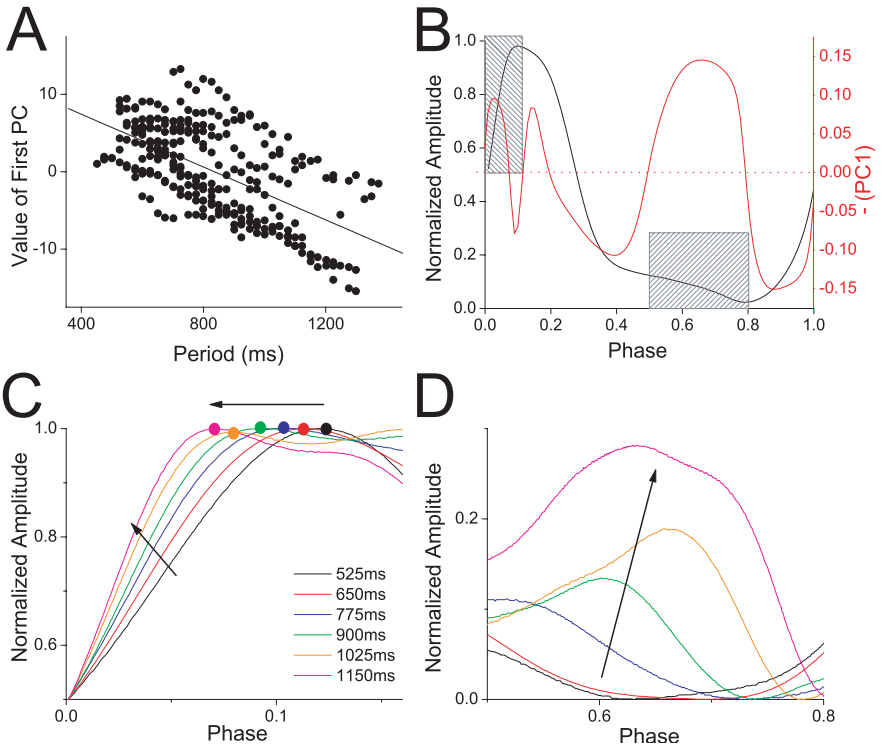

Figure 3. Consistent pattern of change in the LP waveform in response to altering the rhythm period. *A*, The value of the first principal component for all average LP waveforms plotted against the period of the waveform. Linear regression fit shows the high negative correlation between the first PC and the waveform period. *B*, An overlay of the mean of all average waveforms (black line) with the negative of the first PC (red line). The shape of the first PC indicated large variations in the shaded regions of the waveform. *C*, Sections of the LP waveforms from one preparation ranging in period from 525 to 1150 msec. The section shown corresponds to the left shaded box in *B*. Circles show the waveform peaks. The peaks shifted to earlier phases (top arrow), and the trough-to-peak slope became steeper in phase (bottom left arrow) as the period became longer. *D*, Sections of the same waveforms shown in *C* in the region corresponding to the right shaded box in *B*. A second smaller peak started to appear as the waveform period became longer (arrow).

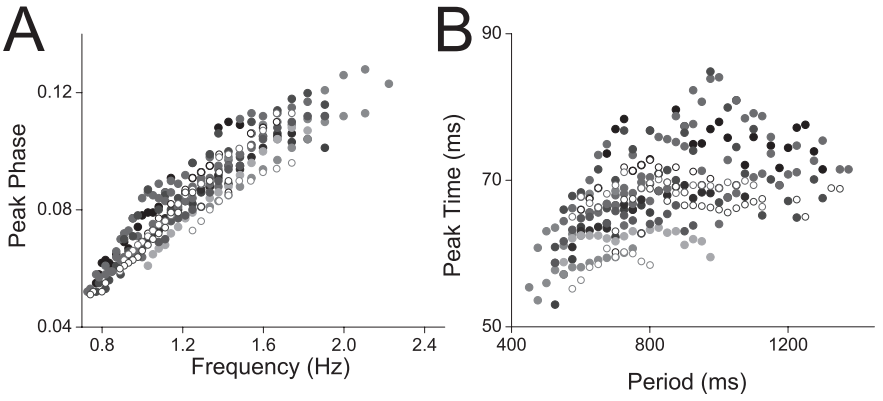

Figure 4. In response to changing the pyloric frequency (period), the peak of the LP waveform is delayed. This shift has a similar proportion across different preparations. *A*, The peak phase of the LP waveform plotted against the frequency of the pyloric rhythm ($n = 14$ preparations). *B*, The peak time of the LP waveform plotted against the period of the pyloric rhythm ($n = 14$ preparations). Different symbols represent different preparations.

An initial comparison of the parameters describing peak (Fig. 4) and initial slope (data not shown) with cycle frequency and cycle period showed that there was some variability in the value of these parameters across preparations even for the same frequency

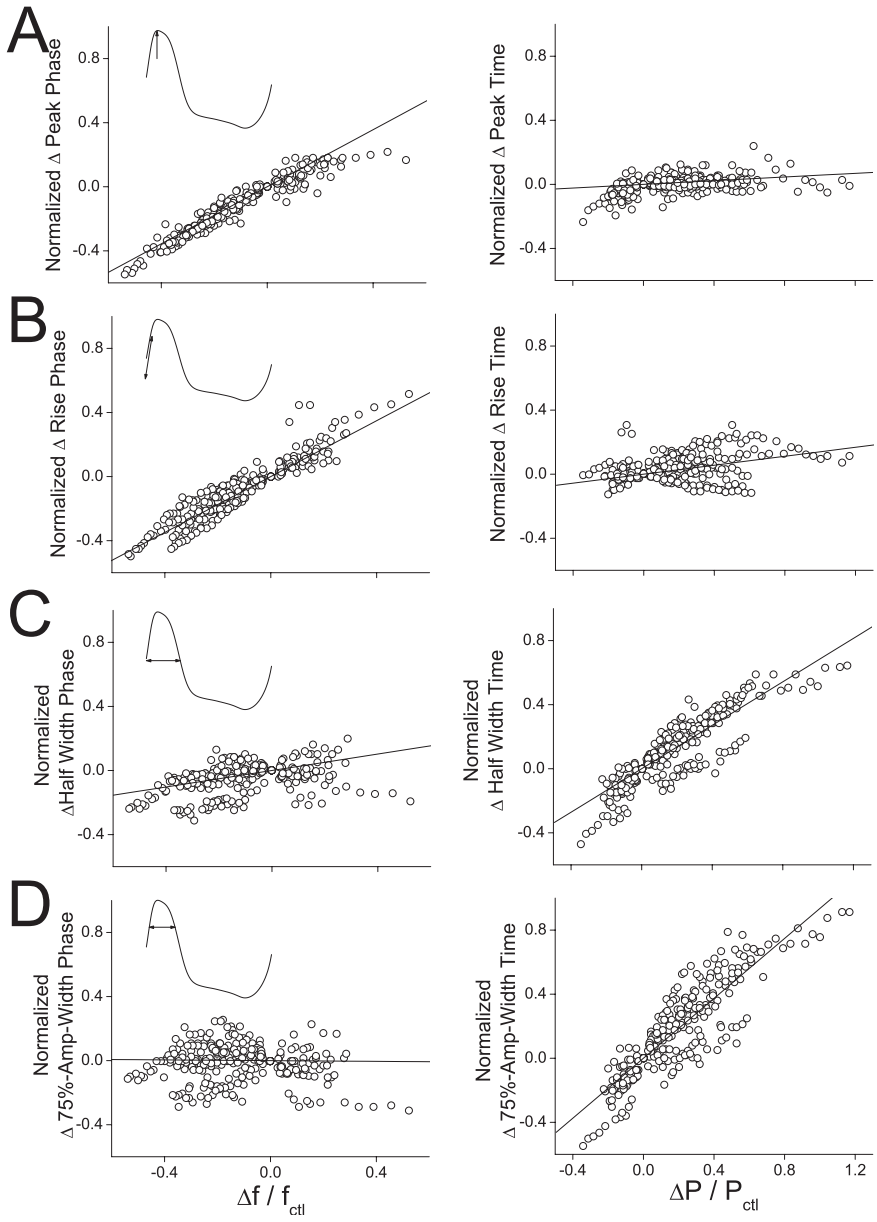

Figure 5. Normalized change in the parameters plotted against the normalized change in the pyloric frequency (period). In the left panels of *A–D*, parameters were measured in phase and plotted against the rhythm frequency. In the right panels, the same parameters were measured in time and plotted against the rhythm period of the pyloric rhythm. The insets of waveforms and arrows in the left panels show the part of the waveform each parameter describes. Linear regression fits are also shown. Parameters shown are the waveform peak (*A*), initial waveform slope (*B*), waveform duty cycle (*C*), and waveform burst width (*D*).

(or period). Interestingly, despite the variability in the actual value of the parameters, it seemed that each parameter from different preparations always changed with a similar trend when the period was changed (Fig. 4). Therefore, instead of comparing the actual parameter values with cycle period, we examined the "sensitivity" of the parameter (X) to changes in frequency f (or period P) (Olsen et al., 1995; Nadim et al., 1998). That is, if the parameter has a value of X_{ctl} at the control frequency f_{ctl} (or the control period P_{ctl}), we measured the fraction of change in the parameter ($\Delta X/X_{ctl}$) when the cycle frequency (or period) is changed by a given fraction ($\Delta f/f_{ctl}$ or $\Delta P/P_{ctl}$). This method of analysis measures the correlation between variations in the parameter ($\Delta X/X_{ctl}$) and variations in frequency ($\Delta f/f_{ctl}$) or period ($\Delta P/P_{ctl}$), as opposed to the correlation between the actual value of the parameter (X) and the actual frequency (f) or period (P).

Figure 5 shows the sensitivity of the parameters describing the LP waveforms to changes in the cycle frequency or period when they are measured in phase (left panels) and in time (right panels). Both the normalized change of peak phase and the initial slope (rise) phase showed a tight positive correlation with the normalized change in frequency (Fig. 5*A*,*B*, left panels) ($r = 0.960$ for peak phase; $r = 0.936$ for slope; $n = 275$; $p < 0.0001$ for both cases). These positive correlations confirmed the previous observation that the waveform peak shifted to earlier phases and the initial slope became steeper in all preparations when the cycle period became longer (cycle frequency became smaller), despite differences in the shape of the waveforms. Moreover, for each parameter, these changes happened at a similar rate across preparations.

When the effect of increasing the cycle period on the peak and initial slope of the waveform was measured in time rather than phase, the trend was in the opposite direction. As cycle period increased, the waveform peak time was delayed and the initial slope (not normalized by period) became less steep. This could be seen as a (weak) positive correlation between both the normalized change in peak time and slope time and the normalized change in period (Fig. 5*A*,*B*, right panels) ($r = 0.429$ for peak time; $r = 0.350$ for slope time; $n = 275$; $p < 0.0001$ for both cases). Linear regression analysis showed that for these two parameters, normalized change in the parameters in response to the normalized change in period was much smaller when the parameters were measured in time (Fig. 5*A*,*B*, right panels) (slopes of 0.0575 and 0.140, respectively), compared with when they were measured in phase (Fig. 5*A*,*B*, left panels) (slopes of 0.890 and 0.872, respectively). These results suggest that when the cycle period is changed, the waveform peak position and the waveform slope followed with more of a constant time delay rather than constant phase. Note that the increase in phase with increasing frequency shown in Figures 4*A* and 5*A* is not contradictory with previous work showing that the LP neuron phase is constant when measured versus the PD neuron burst onset (Hooper, 1997a; Weaver and Hooper, 2003b) because, here, phase is instead being defined relative to the midpoint of the LP neuron rebound depolarization and not relative to the PD neuron.

In contrast to the peak phase and the slope phase of the waveform, the normalized change in duty cycle (as quantified by the waveform half-width) showed only a weak correlation with the normalized change in cycle frequency (Fig. 5*C*, left panel) ($r = 0.396$; $n = 275$; $p < 0.0001$). The correlation between the burst width phase (as quantified by the waveform width at 75% ampli-

tude) and the normalized change in cycle frequency was even weaker (Fig. 5*D*, left panel) ($r = -0.101$; $n = 275$; $p < 0.095$). In contrast, when these features were measured in time, we saw a very high correlation between the normalized change in the parameters and the normalized change in cycle period (Fig. 5*C*,*D*, right panels) ($r = 0.885$ for duty cycle time; $r = 0.882$ for burst width time; $n = 275$; $p < 0.0001$ in both cases). Moreover, linear regression analysis showed that for these two parameters, changes were much larger when the parameter was measured in time (Fig. 5*C*,*D*, right panels) (slopes of 0.678 and 0.935, respectively) than when it was measured in phase (Fig. 5*C*,*D*, left panels) (slopes of 0.257 and −0.011, respectively). Thus, unlike the peak and the slope of the waveform, these parameters changed in a more phase-constant and less time-constant manner when the cycle period was changed.

In most preparations (9 of 14), we saw a second peak develop as the waveform period increased. The six preparations that did not develop the second peak all had a maximum period of <900 msec (the rhythm period did not change much, even when a large hyperpolarizing current was injected in the pacemaker cells). It is possible that the LP waveform would have developed a second peak in these preparations if the rhythm period was long enough. Overall, there was a high correlation between the amplitude of the second peak and the waveform period ($r = 0.611$; $n = 275$; $p < 0.001$; data not shown). However, because in some preparations the waveform did not develop a clear second peak, we did not use the sensitivity measurement to cycle period changes for the second peak amplitude.

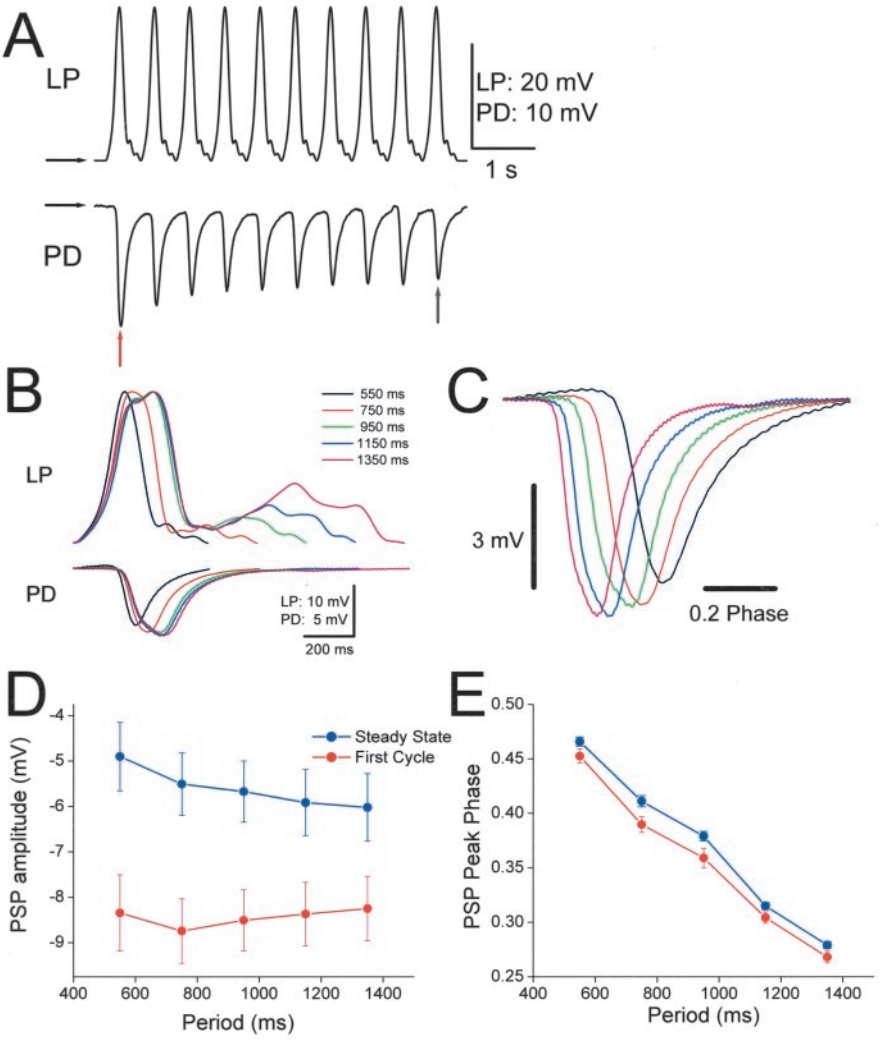

Figure 6. The PSPs in the PD neuron peaks earlier in phase and becomes larger in amplitude as the LP waveform becomes longer. *A*, A trace of the LP neuron voltage clamped with a realistic LP waveform (arrow at −60 mV) and the PSPs recorded from the PD neuron (arrow at −55 mV). *B*, Top, Five LP waveforms with different periods used to activate the synapse. Bottom, Examples of the PSPs in the PD neuron at the tenth cycle (*A*, blue arrow). *C*, The PD neuron PSPs shown in *B* normalized in time. *D*, The amplitude of the PD neuron PSP in response to the first cycle of the LP waveform (red; see red arrow in *A*) and at steady state (blue; average of the last three cycles) plotted against the waveform period. *E*, The peak phase of the PD neuron PSP in response to the first cycle of the LP waveform (red) and at steady state (blue).

How are the PSPs in the PD neuron affected in response to the changes in the LP waveform?

Graded synapses are known to show different responses depending on the shape of the membrane potential waveform of the presynaptic neuron (Olsen and Calabrese, 1996; Manor et al., 1997; Simmons, 2002). Thus, after characterizing how the LP waveform changes in response to changing the cycle period, we investigated how the changes in the LP waveform affected the properties of the LP to PD synapse.

For measuring the PSP in PD neurons, we abolished the ongoing rhythmic activity with bath application of TTX (see Materials and Methods). We then voltage clamped the presynaptic LP neuron,played back the various LP voltage waveforms (corresponding to different rhythm periods) in a rhythmic manner, and recorded the postsynaptic potentials in the PD neurons. Because the LP waveforms differed across preparations but changed with cycle period in a consistent manner, we used only representative waveforms recorded from one preparation. A set of five realistic unitary waveforms corresponding to different pyloric periods was constructed by recording LP voltage traces at different cycle periods, dividing the voltage traces into individual cycles, and low-pass filtering each waveform at 10 Hz (see Materials and Methods) (Fig. 2*A*). Ten repetitions of these unitary waveforms (with a 30 mV trough-to-peak amplitude) were played back into the voltage-clamped LP neuron.

Figure 6*A* shows an example of voltage traces of the LP and PD neurons during the activation of the synapse with 10 repetitions of a realistic waveform corresponding to the cycle period of 550 msec. The top trace shows the voltage-clamped LP neuron, and the lower trace shows the response in the PD neuron. The PSPs in response to the second and subsequent applications of the unitary waveform were smaller than the first PSP, indicating that this synapse shows short-term depression, as shown previously (Manor et al., 1997). The depression of PSP was seen in response to all five waveforms tested, with periods ranging from 550 to 1350 msec (repeated measures two-way ANOVA effect of repeti-

tion on amplitude; $p < 0.0001$). However, the number of cycles needed for the response to reach stable amplitude (steady state) was different for each applied period (repeated measures two-way ANOVA interaction effect between the repetition and the waveform type; $p < 0.0001$). *Post hoc* analysis showed that the amplitude of the PSP stabilized after the sixth cycle for all waveforms (Tukey-Kramer adjusted; $p > 0.05$ after the sixth cycle). Because the pyloric rhythm is normally spontaneously active both *in vivo* and *in vitro*, the synapse should be at its stationary amplitude most of the time, except when the pyloric cycle period is somehow perturbed. We therefore compared the amplitude and the timing of only the steady state PSP in response to different waveforms. We defined the steady state PSP as the average of the PSP in response to the last three cycles of the synapse activation.

Figure 6*B* shows five superimposed waveforms with different periods (550, 750, 950, 1150, and 1350 msec) used to activate the synapse together with the steady state PSP recorded in the PD neuron in response to these waveforms. Note that the longer-period waveforms caused larger-amplitude IPSPs. Furthermore, normalizing the PSP to the cycle period showed that the PSP peak (calculated from the beginning of the LP waveform) shifted to an earlier phase as the waveform period became longer (Fig. 6*C*).

Figure 6*D* shows the average amplitude of PSPs recorded from seven preparations in response to the activation of the synapse by the five LP waveforms (mean ± SEM). We found that although the PSP amplitude in response to the first cycle of the waveform did not depend much on the cycle period of the applied waveform, the steady-state PSP amplitude significantly increased when longer-period LP waveforms were used to activate the synapse (two-way repeated measures ANOVA interaction effect between waveform period and first cycle or steady state, $p < 0.0001$; main effect of the waveform period, $p < 0.0001$; main effect of the cycle, $p < 0.0001$). These results suggested that the increase in amplitude of the steady-state PSP with increased cycle period was mostly attributable to recovery from depression of the PSP when longer waveforms were used to activate the synapse.

Figure 6*E* shows the peak phases of the PSPs (as in Fig. 6*C*) recorded from seven preparations in response to the activation of the synapse by the five different waveforms (mean ± SEM). For both the first cycle PSP and the steady-state PSP, the peak phase advanced significantly as the LP waveform became longer (repeated measures two-way ANOVA; $p < 0.0001$, for the effect of the waveform period on the peak phase). However, there was also a significant interaction between the waveform period effect and the first cycle or steady-state effect on the peak phase of the PSP (repeated measures two-way ANOVA; $p < 0.0047$). Thus, although it was unclear whether the shift in the peak phase was entirely caused by the change of the waveform shape at different periods or also caused by the dynamics of synaptic depression, because the shift was present in the first cycle, it seemed to be determined mostly by the shift in the peak phase of the waveform.

The effect of change in the PSP in the PD neuron on pyloric rhythm period

Thus far, we showed that the steady-state PSP in the PD neuron became larger in amplitude and earlier in phase as the period of the LP waveform used to activate the synapse became longer. In the next step, we examined how these changes in the PSP might in turn affect the pyloric period. Together, these steps followed the effects of changing the rhythm period from the AB-PD neurons to the LP neurons and back around the reciprocally inhibitory loop. To study the effects of the phase and amplitude of the PSP on the pyloric period, we used the dynamic-clamp technique to apply an artificial LP to PD synapse into the PD neuron at different phases of the pyloric rhythm and with different strengths (Fig. 7*A*) (see Materials and Methods). These experiments were performed during an ongoing pyloric rhythm in which the biological LP to PD synapse was removed by hyperpolarizing the LP neuron. The artificial synaptic currents were injected into both PD neurons simultaneously. In each cycle of the PD neuron oscillation, a synaptic conductance of fixed duration and amplitude was applied to the PD neurons. The shape of this conductance was triangular (ramp), approximating the shape of the PSP recorded in the PD neuron (Fig. 6*B*). The triangular synaptic conductance was applied with various peak times to mimic the change in the peak time of the biological synapse (Fig. 6*B*).

Figure 7*B* shows an example of the voltage trace of the PD neuron when a 200 msec triangular artificial synapse (peaking at 100 msec) was applied at four different phases of the PD neuron. The advantage of the triangular shape is that it allows for four

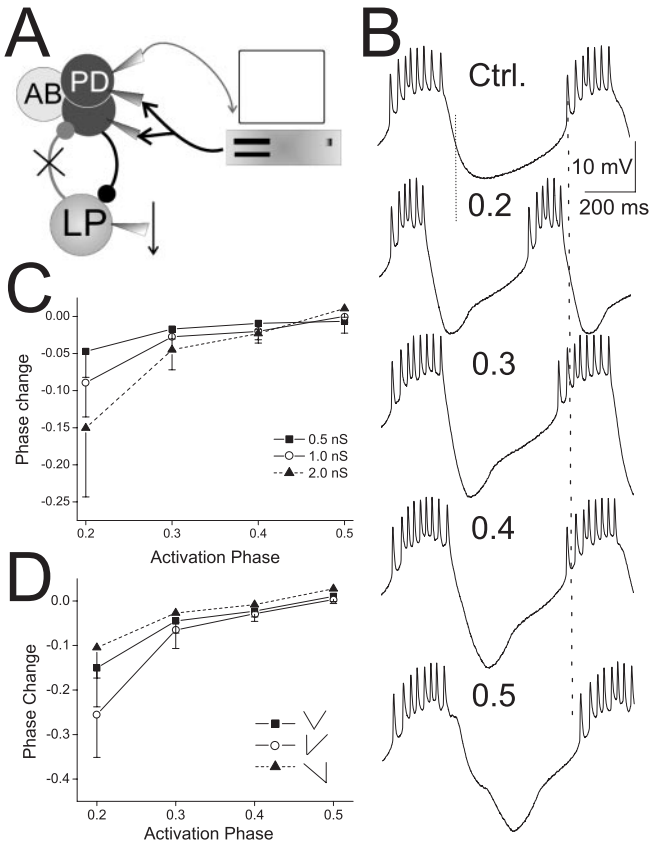

Figure 7. The earlier phase peak and larger amplitude of the PD neuron PSP work to decrease the pyloric rhythm period. *A*, The schematic for the artificial dynamic-clamp synapse experiment. The LP neuron was hyperpolarized to remove the biological LP to PD synaptic current. The artificial synaptic current was calculated using a computer on the basis of preset parameters of the PD neuron membrane potential. The calculated current was injected into both PD neurons through intracellular electrodes. *B*, An example of the voltage traces of the PD neuron in control (Ctrl.; no injection) and in response to the artificial LP to PD synapse activated at different phases of the oscillation cycle. Vertical dotted lines indicate the beginning of the bursts of the control trace. *C*, The phase change in the PD neuron $[(P_{\text{during injection}} - P_{\text{ctl}})/P_{\text{ctl}}]$ is shown in response to the activation of the artificial synapse with different strengths and at different phases of the cycle. Increasing the artificial synaptic conductance injected at an early phase increased the extent of the phase change in the PD neuron. For clarity, only negative error bars are shown. *D*, An earlier peak of the artificial synaptic conductance (peak at 0, 100, and 200 msec in each cycle) also increased the extent of the phase change in the PD neuron. For clarity, only negative error bars are shown.

parameters that could be changed independently. These parameters are duration, amplitude, phase (with reference to PD), and peak time. We varied the phase of the artificial synapse in a range similar to that of the PD neuron PSP phase in response to the LP waveform activation. The duration was kept constant at 200 msec, similar to that of the PD neuron PSP, and the conductance amplitudes were chosen empirically to produce an IPSP in the PD neuron that was comparable in size with that of the biological LP to PD synapse. The peak time was changed from zero to midpoint to maximum duration of the synapse.

The activation of the synapse at an early phase shortened the rhythm period compared with the control period. As the activation phase of the synapse was increased, the cycle period became longer such that at phase 0.5, the activation of the synapse increased the period compared with the control period (Fig. 7, dotted vertical lines). Figure 7*C* shows the summary of the average phase change (mean $\pm \sigma$; $n = 7$ preparations) in response to the activation of the artificial synapse with different strengths (0.5, 1.0, and 2.0 nS) and phases (0.2, 0.3, 0.4, 0.5). The change in the period (P) is shown as a phase change in the PD neuron $(P_{\text{during injection}} - P_{\text{ctl}})/P_{\text{ctl}}$. Although the amount of phase change varied across preparations, in all preparations, the synapse injected at an earlier phase shortened the cycle period, and increasing the synaptic strength enhanced this effect (repeated measures two-way ANOVA; main effect of the phase, $p < 0.0001$, and the strength, $p < 0.0008$). The interaction between phase and strength was also statistically significant (repeated measures two-way ANOVA, $p < 0.0002$), suggesting that the increase in the synaptic strength had a larger effect on the rhythm period when the synapse was activated at an earlier phase.

Figure 7*D* shows the average phase change in response to the artificial synapse with different peak times (0, 100, and 200 msec) injected at four phases (0.2, 0.3, 0.4, and 0.5; mean $\pm \sigma$; $n = 6$ preparations). The phase change was consistently more negative when the synapse peaked earlier in time (repeated measures two-way ANOVA; main effect of the peak time, $p < 0.0038$; interaction between the peak time and the phase not statistically significant, $p > 0.11$). These data suggest that the peak time of the synapse can be important in determining its effect on the rhythm period.

Summary of results

This study was done in three sets of experiments. First, we showed that the membrane potential waveform of the LP neuron changed according to a consistent pattern in response to altering the pyloric period. Notable changes included a shift of the initial peak to earlier phases, an increase in the initial slope in phase, and a second smaller peak appearing as the rhythm period became longer. In the second set of experiments, we showed that these changes affect the dynamics of the LP to PD synapse by causing the PSP in the PD neuron to peak earlier in phase and become larger in amplitude. Finally, using an artificial LP to PD synapse, we showed that PSPs occurring at an earlier phase can speed up the rhythm, and larger PSPs can also strengthen this trend.

These results suggest that the LP to PD synapse dynamically changes its properties to provide a negative feedback that tends to stabilize the rhythm period, at least when the period is increased. The effect of this negative feedback loop is best described in response to a perturbation that increases the rhythm period. Whenever the period of the rhythm is increased, the shape of the LP waveform changes in a consistent manner. The change in the shape of the LP waveform causes a change in the amplitude and peak time of the LP to PD synapse, providing a feedback that opposes the initial change in period.

Discussion

We used the lobster pyloric network to investigate the dynamic interaction between two oscillatory neurons, a pacemaker and a follower, connected with reciprocally inhibitory synapses. These experiments indicated that interactions between pacemaker and follower neurons dynamically respond to changes in the rhythm period and thus provide a negative feedback mechanism, which could work to stabilize the rhythm period if the period is altered.

Possible mechanisms underlying changes in the LP waveform

The pyloric rhythm can maintain its pattern over a wide range of frequencies (Hooper, 1997a). Various mechanisms have been suggested to play a role in phase maintenance of the burst onset (or termination) of some pyloric neurons measured in reference to the pyloric pacemakers (Harris-Warrick et al., 1995; Hooper et al., 2002; Manor et al., 2003; Nadim et al., 2003). Of the LP neuron waveform parameters measured in the current study, the peak time and rise slope are most likely attributable to intrinsic properties of the LP neuron. These parameters determine the burst latency of the LP neuron (in reference to AB–PD). Because neither of these parameters (in time units) changed with period, the phase maintenance of the LP neuron burst onset relative to the PD neuron as observed in the intact network (Hooper, 1997a; Weaver and Hooper, 2003b) is most likely attributable to synaptic effects (e.g., longer PD–AB neuron bursts and possible changes in the duration of the inhibition they induce in the LP neuron as cycle period increases). This is in contrast to the pyloric constrictor (PY) neurons, which change their waveform to depolarize more rapidly and thus recover from inhibition more quickly as a partial mechanism to maintain their phase in the pyloric pattern as cycle period decreases (Hooper, 1998). In contrast, the LP burst width remains almost constant in phase. One mechanism that may control the LP burst width is the inhibitory synaptic input from the PY neurons that act to terminate the LP burst. In fact, previous studies have shown that the PY burst phase relative to the LP burst is kept almost constant over a wide range of pyloric periods (Hooper, 1997a,b). This mechanism is also consistent with the results of a previous study in which we showed that the LP to PY synapse might help maintain a constant phase difference between these two neurons (Mamiya et al., 2003). Thus, the changes in the timing of both the onset and the end of the LP neuron activity necessary to maintain phase are apparently caused by varying synaptic input and not to changes in LP neuron intrinsic properties.

The effect of changes in the LP waveform on the PSP in the PD neuron

The amplitude of the PSP in the PD neuron in response to the first cycle of the LP waveform was similar for all waveform periods. Several studies have shown that the slope of presynaptic membrane potential plays an important role in determining the amplitude of graded synapses (Olsen and Calabrese, 1996; Manor et al., 1997; Simmons, 2002). Thus, it is not surprising that the LP waveforms, which have similar slopes (measured in time), produce similar PSP amplitudes. In contrast, the amplitude of the steady-state PSPs became larger as the period was increased. This suggests that the shape and period of the presynaptic waveform influenced the amount of synaptic depression and, overall, longer LP waveforms allowed better recovery of the synapse.

In contrast to amplitude, the peak phase of the PD neuron

PSPs varied greatly in response to LP waveforms with different periods, even in the first cycle. This variation seemed to be mostly because of the large difference in the peak phase of the LP waveforms at different periods. The peak phase of the PSP in response to each type of LP waveform changed only slightly between the initial cycle and the steady state. Thus, the influence of synaptic depression on the peak phase of the PSP was small compared with the large difference in the peak phase of different LP waveforms.

The effect of changes in the PD neuron PSP on the rhythm period

To examine the effect of the LP to PD synapse on the pyloric period, we used artificial synaptic inputs with a simplified triangular (ramp) conductance in each cycle. The tendency of the synapse activated at an earlier phase was to shorten the period, and this tendency was consistent for all peak times and amplitudes, although the synapse with an early peak time or larger amplitude was more effective in reducing the period. A previous study of the phase response curve of PD neurons in the lobster *Homarus americanus* also showed similar results (Prinz et al., 2003). The unexpected shortening of the rhythm period by an inhibitory synapse is probably attributable to both the early termination of the PD burst by the synapse and the activation of an inward current by the inhibitory synapse resulting in a faster postinhibitory rebound. However, other mechanisms cannot be ruled out without additional experiments. Within the range of conductances tested, the effect on the rhythm period was larger with a larger conductance. This contrasts with the results of Prinz et al. (2003) that the effect of increasing synaptic conductance saturates. However, the difference is most likely attributable to the range of conductance tested. The IPSPs produced by our artificial synapse were in the range of 0.5–5 mV, comparable with the IPSPs observed for the biological synapse under control conditions. It is possible that the saturation effect seen by Prinz et al. (2003) is applicable for a much stronger synapse, which may occur under certain modulatory conditions (Johnson and Harris-Warrick, 1990, 1997).

One way of examining our hypothesis that the LP to PD synapse acts to reduce the pyloric cycle period when the period is increased is to eliminate the synapse. In a previous study, a set of experiments was done that functionally removed the LP to PD synapse (Weaver and Hooper, 2003a). This study suggested that the LP to PD synapse always acts to increase the pyloric cycle period. However, these results may be confounded by the fact that the LP neuron also has a synapse to another pyloric neuron (VD), which might affect the pyloric period through its electrical coupling to the pacemakers (Weaver and Hooper, 2003a). Indeed, our preliminary results show that when the VD neuron is inactivated, the removal of the LP to PD synapse can slow the rhythm period. Additional experiments are needed to confirm this effect.

It is also important to note that there is range of phase values (0.4–0.5) in which the changes in strength (within the range tested) or phase of the artificial synapse has a limited effect on the pyloric cycle period. This insensitive range might help provide local flexibility to the pyloric rhythm while maintaining overall stability of the rhythm. For example, if the pyloric period is within this range, the pacemaker group can vary the cycle period readily without any effect from the feedback synapse. Only when the period becomes too long or too short the feedback synapse works to oppose the change and stabilize the period. Interestingly, this negative feedback would also work to bring the LP neuron burst phase (relative to the pacemakers) to the insensitive range, thus providing overall stability of the LP neuron burst. The coexistence of local flexibility and overall stability might be important for the proper operation of the pyloric circuit, which is known to produce various types of patterns with various periods.

Summary

Recent computational studies have suggested that oscillatory neurons connected with reciprocally inhibitory depressing synapses should show bistability (Nadim et al., 1999; Manor and Nadim, 2001). The two stable oscillations are a fast rhythm in which the synapses are maximally depressed and a slower rhythm in which they are maximally recovered from depression. The network could switch from one state to another in response to a brief perturbation of period. However, such bistability has not been observed in the biological pyloric network, and results from the present study suggest that the positive feedback loop necessary for the bistability may not exist. The change in the waveform shape and the resulting change in the shape and amplitude of the PSP act to provide a negative rather than a positive feedback and help maintain the rhythm period in a stable state. However, note that our results do not completely rule out the possibility of bistability.

It would be interesting to see whether other oscillatory networks involving reciprocal inhibition have similar compensatory mechanisms that act to stabilize the rhythm period. It is also important to explore the possibility that different neuromodulators might modify this stabilization mechanism to control the period more effectively. For example, under certain modulatory conditions, the negative feedback might be removed or adjusted to allow for an increase or decrease in the rhythm period. Such modulatory mechanisms would allow a more gradual and flexible control of the rhythm produced by the network.

References

Brody DL, Yue DT (2000) Relief of G-protein inhibition of calcium channels and short-term synaptic facilitation in cultured hippocampal neurons. J Neurosci 20:889–898.

Freund TF, Buzsaki G (1996) Interneurons of the hippocampus. Hippocampus 6:347–470.

Glaser EM, Ruchkin DS (1976) Principles of neurobiological signal analysis. New York: Academic.

Graubard K (1978) Synaptic transmission without action potentials: input-output properties of a nonspiking presynaptic neuron. J Neurophysiol 41:1014–1025.

Harris-Warrick RM, Coniglio LM, Levini RM, Gueron S, Guckenheimer J (1995) Dopamine modulation of two subthreshold currents produces phase shifts in activity of an identified motoneuron. J Neurophysiol 74:1404–1420.

Hooper SL (1997a) Phase maintenance in the pyloric pattern of the lobster (Panulirus interruptus) stomatogastric ganglion. J Comput Neurosci 4:191–205.

Hooper SL (1997b) The pyloric pattern of the lobster (Panulirus interruptus) stomatogastric ganglion comprises two phase-maintaining subsets. J Comput Neurosci 4:207–219.

Hooper SL (1998) Transduction of temporal patterns by single neurons. Nat Neurosci 1:720–726.

Hooper SL, Buchman E, Hobbs KH (2002) A computational role for slow conductances: single-neuron models that measure duration. Nat Neurosci 5:552–556.

Johnson BR, Harris-Warrick RM (1990) Aminergic modulation of graded synaptic transmission in the lobster stomatogastric ganglion. J Neurosci 10:2066–2076.

Johnson BR, Harris-Warrick RM (1997) Amine modulation of glutamate responses from pyloric motor neurons in lobster stomatogastric ganglion. J Neurophysiol 78:3210–3221.

Kisvarday ZF, Beaulieu C, Eysel UT (1993) Network of GABAergic large basket cells in cat visual cortex (area 18): implication for lateral disinhibition. J Comp Neurol 327:398–415.

Lewis JE, Maler L (2002) Dynamics of electrosensory feedback: short-term plasticity and inhibition in a parallel fiber pathway. J Neurophysiol 88:1695–1706.

Mamiya A, Manor Y, Nadim F (2003) Short-term dynamics of a mixed chemical and electrical synapse in a rhythmic network. J Neurosci 23:9557–9564.

Manor Y, Nadim F (2001) Synaptic depression mediates bistability in neuronal networks with recurrent inhibitory connectivity. J Neurosci 21:9460–9470.

Manor Y, Nadim F, Abbott LF, Marder E (1997) Temporal dynamics of graded synaptic transmission in the lobster stomatogastric ganglion. J Neurosci 17:5610–5621.

Manor Y, Bose A, Booth V, Nadim F (2003) The contribution of synaptic depression to phase maintenance in a model rhythmic network. J Neurophysiol.

Marder E, Calabrese RL (1996) Principles of rhythmic motor pattern generation. Physiol Rev 76:687–717.

Nadim F, Manor Y, Nusbaum MP, Marder E (1998) Frequency regulation of a slow rhythm by a fast periodic input. J Neurosci 18:5053–5067.

Nadim F, Manor Y, Kopell N, Marder E (1999) Synaptic depression creates a switch that controls the frequency of an oscillatory circuit. Proc Natl Acad Sci USA 96:8206–8211.

Nadim F, Booth V, Bose A, Manor Y (2003) Short-term synaptic dynamics promote phase maintenance in multi-phasic rhythms. Neurocomput 52–54:79–87.

Olsen ØH, Calabrese RL (1996) Activation of intrinsic and synaptic currents in leech heart interneurons by realistic waveforms. J Neurosci 16:4958–4970.

Olsen ØH, Nadim F, Calabrese RL (1995) Modeling the leech heartbeat elemental oscillator. II. Exploring the parameter space. J Comput Neurosci 2:237–257.

Prinz AA, Thirumalai V, Marder E (2003) The functional consequences of changes in the strength and duration of synaptic inputs to oscillatory neurons. J Neurosci 23:943–954.

Rabbah PM, Atamturktur S, Nadim F (2002) Distinct synaptic dynamics by the pacemaker neurons of a rhythmic neuronal network. Soc Neurosci Abstr 28:752.5.

Raper JA (1979) Nonimpulse-mediated synaptic transmission during the generation of a cyclic motor program. Science 205:304–306.

Selverston AI, Russell DF, Miller JP (1976) The stomatogastric nervous system: structure and function of a small neural network. Prog Neurobiol 7:215–290.

Sharp AA, O'Neil MB, Abbott LF, Marder E (1993) The dynamic clamp: artificial conductances in biological neurons. Trends Neurosci 16:389–394.

Simmons P (2002) Presynaptic depolarization rate controls transmission at an invertebrate synapse. Neuron 35:749–758.

Skinner FK, Kopell N, Marder E (1994) Mechanisms for oscillation and frequency control in reciprocal inhibitory model neural networks. J Comput Neurosci 1:69–87.

Taylor AL, Cottrell GW, Kristan Jr WB (2002) Analysis of oscillations in a reciprocally inhibitory network with synaptic depression. Neural Comput 14:561–581.

Van Vreeswijk C, Abbott LF, Ermentrout GB (1994) When inhibition not excitation synchronizes neural firing. J Comput Neurosci 1:313–321.

Wang X-J, Rinzel J (1992) Alternating and synchronous rhythms in reciprocally inhibitory model neurons. Neural Comp 4:84–97.

Weaver AL, Hooper SL (2003a) Follower neurons in lobster (Panulirus interruptus) pyloric network regulate pacemaker period in complementary ways. J Neurophysiol 89:1327–1338.

Weaver AL, Hooper SL (2003b) Relating network synaptic connectivity and network activity in the lobster (Panulirus interruptus) pyloric network. J Neurophysiol 90:2378–2386.